Michigan Technological University

Michigan Technological University
Digital Commons @ Michigan Tech

Department of Physics Publications | Department of Physics

2-1-1994

The use of optimal polarizations for studying the microphysics of precipitation: Nonattenuating wavelengths

John Kwiatkowski
Michigan Technological University

Alexander Kostinski
Michigan Technological University

A. R. Jameson
RJH Scientific, Inc.

Follow this and additional works at: https://digitalcommons.mtu.edu/physics-fp

 Part of the Physics Commons

Recommended Citation

Kwiatkowski, J., Kostinski, A., & Jameson, A. R. (1994). The use of optimal polarizations for studying the microphysics of precipitation: Nonattenuating wavelengths. *Journal of Atmospheric and Oceanic Technology, 12*(1), 96-114. http://dx.doi.org/10.1175/1520-0426(1995)012<0096:TUOOPF>2.0.CO;2
Retrieved from: https://digitalcommons.mtu.edu/physics-fp/258

Follow this and additional works at: https://digitalcommons.mtu.edu/physics-fp

 Part of the Physics Commons

The Use of Optimal Polarizations for Studying the Microphysics of Precipitation: Nonattenuating Wavelengths

JOHN M. KWIATKOWSKI AND ALEXANDER B. KOSTINSKI

Department of Physics, Michigan Technological University, Houghton, Michigan

A. R. JAMESON

Applied Research Corporation, Landover, Maryland

(Manuscript received 7 June 1993, in final form 15 June 1994)

ABSTRACT

The objective of this work is to explore relationships between the microphysical properties of precipitation and optimal polarizations. The dependence of three optimal polarization parameters (asymmetry ratio $\mathcal{A}$, optimal tilt τ_{op}, and optimal ellipticity ϵ_{op}) on the reflectivity-weighted mean drop shape, mean canting angle, and standard deviation of a Gaussian canting angle distribution is studied. This is accomplished by using computer simulations that provide the rms scattering matrix for an ensemble of canted drops with a prescribed two-parameter canting angle distribution. Also examined are the effects of propagation on the polarization parameters for nonattenuating wavelengths.

The asymmetry ratio $\mathcal{A}$ is simply the ratio of the maximal to minimal total backscattered energy (ratio of the largest and smallest eigenvalue of the Graves power matrix $\mathbf{G} = \mathbf{S}^{\dagger}\mathbf{S}$). Similar to Z_{DR}, this ratio decreases with increasing mean axial ratio, but unlike Z_{DR}, it is not affected by canting (for a single drop). The dependence of $\mathcal{A}$ on the reflectivity-weighted mean drop shape is examined, and a power-law relationship similar to that which exists for Z_{DR} is established. The asymmetry ratio $\mathcal{A}$ can be regarded as a generalization of Z_{DR} because it requires only a measurement of linear depolarization ratio (in addition to Z_{DR}), is independent of the propagation phase, and is less sensitive to canting. In a similar manner, the dependence of optimal ellipticity and tilt on the microphysical parameters is studied. In particular, it appears that the rms tilt of the optimal polarization ellipse is proportional to the variance of the canting angle distribution. Several other promising relationships between optimal polarizations and the microphysical variables of an ensemble of hydrometeors are also discussed.

1. Introduction

The usefulness of polarimetric methods in radar sensing of precipitation has been demonstrated not only in numerous recent articles (Zrnić et al. 1993; Holt 1992; Hubbert et al. 1993; Vivekanandan et al. 1991; Aydin and Zhao 1990) but in recent textbooks and monographs as well (Doviak and Zrnić 1993; Sauvageot 1992; Bringi and Hendry 1990; Jameson and Johnson 1990). Polarimetric quantities such as CDR (circular depolarization ratio) (McCormick and Hendry 1975), Z_{DR} (differential reflectivity) (Seliga and Bringi 1976), LDR (linear depolarization ratio) (e.g., Battan 1973), propagation differential phase (Seliga and Bringi 1978; Jameson 1985b), and time series of the polarimetric quantities (Bringi et al. 1983) have been used to deduce microphysical parameters from radar measurements. There seems to be a trend toward increasingly sophisticated polarimetric signatures in an attempt to recover the microphysics of the precipitation. For instance, a recent article by Hubbert et al. (1993) is devoted mostly to separation of backscatter and propagation differential phases. Motivated by this trend, this work focuses on the following general question: What additional microphysical information is contained in the full polarization scattering matrix $\mathbf{S}$? Thus, the purpose of this research is to develop a systematic methodology to search for new polarimetric signatures.

In order to understand the microphysical information contained in the polarization scattering matrix, we choose to examine its eigenvalues and eigenvectors. This is a natural choice for several reasons. First of all, eigenvectors and eigenvalues contain the same information as the matrix itself, but it is in a form that allows separation of the orientation-invariant quantities. For example, the eigenvalues (and their combinations, e.g., trace and determinant) are invariant with respect to rotations performed on $\mathbf{S}$. This may allow separation of shape and canting effects, thereby providing an easier interpretation of the microphysical parameters. Eigenvalue computations for a 2×2 matrix

Corresponding author address: John Kwiatkowski, Physics Department, Michigan Technological University, 1400 Townsend Drive, Houghton, MI 49931.

© 1995 American Meteorological Society

involve only quadratic equations and can be performed simply and in real time. Also, there is an appealing physical interpretation that relates the eigenvalues and eigenvectors of the Graves power matrix $\mathbf{G} = \mathbf{S}^{\dagger}\mathbf{S}$ (Graves 1956) ("†" denotes Hermitian adjoint) to extrema of total backscattered energy and to the transmitted polarizations corresponding to these extrema (Kostinski and Boerner 1986; Ishimaru 1991, p. 506). Furthermore, the eigenvectors can be expressed in the form of two parameters of the polarization ellipse (ellipticity and tilt), which separate shape and orientation on the level of the wave itself (Born and Wolf 1980; Azzam and Bashara 1977). Thus, the objective of this work is to explore how the physical properties of precipitation such as the canting angle distribution of hydrometeors, their shape, etc., affect the eigenpolarizations of the Graves power matrix $\mathbf{G} = \mathbf{S}^{\dagger}\mathbf{S}$.

In order to gain insight into the dependence of optimal polarizations on microphysical parameters, we concentrate on a familiar form of precipitation: rain. The rain drops are modeled as oblate spheroids, and scattering amplitudes can be calculated numerically (e.g., see section 4a where the T-matrix method is used). Calculations have been performed for S band that provide the scattering matrix as a function of several microphysical parameters, including mean axial ratio (through the rain rate), the mean and standard deviation of a one-dimensional canting angle distribution, and the rate of propagation differential phase shift. The S band was chosen because the backscatter phase shift and attenuation due to propagation can be ignored. (See appendix D for possible effects of differential attenuation.)

This paper is an attempt to explore the connection between the microphysical parameters of an ensemble of hydrometeors—for example, canting angle distribution, mean axial ratio, propagation differential phase shift, and optimal polarization parameters defined below. Although rain has been chosen as our test media, our goal is to explore the dependence of the new polarization parameters on the characteristics of precipitation in general. Therefore, the microphysical parameters are pushed to values that one would not normally find in rain but that might occur in other forms of precipitation.

In the following section, specific background information is given on the polarimetric variables, their relationship to microphysical parameters, and the basic theory behind the calculations for the scattering matrix for a single raindrop and for an ensemble of drops.

2. Background

For the sake of completeness, some basic definitions of radar polarimetry used in this paper are included in appendix A. For the reader's convenience the optimal polarization approach is briefly reviewed next.

a. Optimal polarizations

The eigenpolarization approach used here and described in Kostinski and Boerner (1986) and Ishimaru (1991, p. 506) is based on the consideration of extrema of *total* backscattered energy as a function of transmitted polarization. The method results in an eigenvalue problem for a Hermitian power (Graves) matrix (Graves 1956):

$$\mathbf{G} \equiv \mathbf{S}^{\dagger}\mathbf{S},$$

where $\mathbf{S}$ is the complex scattering matrix (see appendix A). The eigenvalues of $\mathbf{G}$ are always real and equal to the maximum and minimum of scattered powers, while the eigenvectors are the corresponding polarization states of the transmitted wave. The optimal polarization is defined to be that *transmitted* polarization that maximizes (minimizes) the *total backscattered* intensity in free space.[1] Note that the emphasis here is on retrieving microphysics not on radar reception. The optimal polarization gives the maximum total backscattered energy in free space, and this wave can still be (mis)matched at the receiving antenna (e.g., Collin 1985, p. 303).

The solutions to the eigenvalue problem

$$\mathbf{G}x = \lambda x$$

are the polarization vectors $\mathbf{E}_1$, $\mathbf{E}_2$ (eigenvectors) and the scattered powers λ_1, λ_2 (eigenvalues) of the maximal (minimal) transmit polarizations. From $\mathbf{E}_1$ and $\mathbf{E}_2$, we calculate the ellipticity ϵ and tilt τ of the polarization ellipse, which yields the maximum (minimum) scattered power. The ellipticity and tilt of the maximum eigenvector (the eigenvector associated with the maximal eigenvalue) are labeled as ϵ_{op} and τ_{op}, respectively. The ratio of the maximal to minimal eigenvalues (asymmetry ratio) is denoted as $\mathcal{A} \equiv \lambda_1/\lambda_2$. The variables $\mathcal{A}$, ϵ_{op}, and τ_{op} are the polarization parameters that are examined in this paper.

b. Connection to precipitation microphysics

We now describe the scattering of completely polarized waves from a volume of precipitation and relate the microphysics of precipitation to elements of the scattering matrix. The scattering matrix in its normalized form is

$$\mathbf{S} = \begin{bmatrix} 1 & be^{i\gamma} \\ be^{i\gamma} & ae^{i\delta} \end{bmatrix}, \tag{1}$$

where a and b are magnitudes equal to $|S_{VV}|/|S_{HH}|$ and $|S_{VH}|/|S_{HH}|$, respectively (see appendix A for details).

[1] This technique has been used for determining polarizations that enhance contrast in radar imaging (Kostinski et al. 1988).

The phase differences in the normalized scattering matrix (1) have specific physical significance in precipitation. Differential phase shifts can be produced by two mechanisms: scattering and propagation. The differential phase shifts due to *backscatter* are defined as δ for the copolarized and γ for the cross-polarized components in the scattering matrix. Therefore (1) can represent scattering from a single drop or an ensemble of drops while neglecting propagation effects.

As a wave propagates through a volume of precipitation, the propagation differential phase shift between the vertical and horizontal polarized components ϕ is given as twice the rate of (or specific) propagation differential phase shift Φ (relative to *HH*) times the one-way propagation distance L; that is, $\phi = 2L\Phi$. The propagation differential phase shift for the cross-polarized components in **S** is one-half that of the copolarized phase shift (Doviak and Zrnić 1993, p. 244). The scattering matrix of an ensemble of scatterers including propagation effects is then written as

$$\mathbf{S} = \begin{bmatrix} 1 & be^{i(\gamma+\phi/2)} \\ be^{i(\gamma+\phi/2)} & ae^{i(\delta+\phi)} \end{bmatrix}. \tag{2}$$

Note that since the matrix is normalized by the *HH* element, the differential phase is defined as $\phi = \phi_{VV} - \phi_{HH}$.

In this paper, we restrict ourselves to nonattenuating wavelengths. For our test case we choose S band (2.80 GHz, λ = 10.7 cm). At this wavelength, several simplifications to the scattering matrix (2) can be made. Both differential phase shifts due to backscatter (δ and γ) can be generally ignored in rain at this frequency, because even in the heaviest rain δ does not exceed 1°. Attenuation, in general, can be ignored at this wavelength as well (Bringi and Hendry 1990). (See appendix D for possible effects of differential attenuation.) Therefore, the only effect of propagation is the accumulation of propagation differential phase shift ϕ. The simplified scattering matrix can now be written as

$$\mathbf{S} = \begin{bmatrix} 1 & be^{i(\phi/2)} \\ be^{i(\phi/2)} & ae^{i(\phi)} \end{bmatrix}. \tag{3}$$

Having introduced the optimal polarization quantities $\mathcal{A}$, τ_{op}, and ϵ_{op}, the next step is to determine what information they contain about the size, shape, and orientation of the scatterers. As was mentioned in the introduction, the motivation for using the eigen-polarization approach as opposed to other polarization quantities such as Z_{DR} (log ratio of horizontal to vertical radar returns) is rotational invariance. For instance, for a single drop, the asymmetry ratio $\mathcal{A}$ (a function of eigenvalues) decreases as the drop axial ratio increases, as does Z_{DR}; however, it is independent of rotations (e.g., Strang 1988, p. 304) performed on the scattering matrix, unlike Z_{DR}. This fact is likely to help in retrieval of canting parameters as well. Indeed, canting of hydrometeors has been examined in (Holt 1984; Aydin and Zhao 1990; Jameson 1985a) using rotation matrices acting on **S**.

Thus, our focus is on the dependence of the three optimal polarization quantities $\mathcal{A}$, ϵ_{op}, and τ_{op} on four microphysical parameters of an ensemble of raindrops: reflectivity-weighted mean axial ratio $\mathcal{R}$, the mean canting angle $\bar{\beta}$, the standard deviation of the canting angle distribution σ_β, and the propagation differential phase shift ϕ.

To gain basic physical insight into the dependence of the polarization parameters on the microphysical properties of raindrops, we begin with a single drop and then extend the discussion to an ensemble of drops. The drop shape used in this work is that of an oblate spheroid, but the results for a single drop as stated in section 3 are valid for a more general class of particles (with perpendicular symmetry planes). In the next section, the dependence of $\mathcal{A}$, ϵ_{op}, and τ_{op} on the scattering matrix of a single canted hydrometer is studied in some detail (before discussing the ensemble case) in order to establish a physical connection between the optimal polarization parameters and the drop characteristics.

3. Single-canted hydrometeor

In the single drop case, it is expected by symmetry that the polarization that maximizes the scattered power is along the major axis of the drop. This is easily visualized in the Rayleigh region,[2] where the drop can be thought of as composed of two simultaneously oscillating dipoles along the principal axes. A linearly polarized wave aligned along the longer principal axis of the drop is then associated with the strongest echo. It is shown below that this conclusion remains valid in the Mie region.

In this section the solution to the optimal polarization problem for a single spheroidal hydrometeor is presented. For simplicity of interpretation, the hydrometeors are constrained to cant only in the plane of polarization throughout the rest of this paper. When the drop is aligned with its symmetry axis along the local horizontal and vertical (the polarization basis used here), the scattering matrix is diagonal (e.g., van de Hulst 1981; Bohren and Huffman 1983) and can be written as

$$\mathbf{S}^0 = \begin{bmatrix} S^0_{HH} & 0 \\ 0 & S^0_{VV} \end{bmatrix}, \tag{4}$$

where the principal plane complex scattering amplitudes and the matrix are denoted with a superscript 0.

[2] The term Rayleigh scattering is used here when the particle size is sufficiently small compared to the wavelength so that two orthogonally polarized incident waves induce dipoles oscillating in phase with the incident field. In this region no differential phase shift can occur (for a single particle).

Following standard matrix techniques (e.g., Strang 1988, p. 167) as well as several meteorological investigations (van de Hulst 1981; Holt 1984; Aydin and Zhao 1990), a single symmetrical scatterer canting in the plane of polarization (Fig. 1) can be described by a rotation operation on the principal plane scattering matrix $\mathbf{S}^0$. The rotation operator $\mathbf{R}$ with canting angle β is given as

$$\mathbf{R} = \begin{bmatrix} \cos\beta & -\sin\beta \\ \sin\beta & \cos\beta \end{bmatrix}.$$

The scattering matrix for a canted hydrometeor can then be expressed as

$$\mathbf{S} = \mathbf{R}^{-1}\mathbf{S}^0\mathbf{R} = \begin{bmatrix} S_{HH} & S_{HV} \\ S_{VH} & S_{VV} \end{bmatrix}. \quad (5)$$

This scattering matrix represents the particle at an arbitrary orientation in the plane of polarization. The elements of $\mathbf{S}$ become

$$S_{HH} = S^0_{HH}\cos^2\beta + S^0_{VV}\sin^2\beta \quad (6)$$

$$S_{HV} = S_{VH} = (S^0_{VV} - S^0_{HH})\cos\beta\sin\beta \quad (7)$$

$$S_{VV} = S^0_{HH}\sin^2\beta + S^0_{VV}\cos^2\beta. \quad (8)$$

The quantities S^0_{HH} and S^0_{VV} are the principal plane complex scattering amplitudes and β is the canting angle in the plane of polarization. The canting angle β is taken to be positive clockwise from the vertical axis while looking at the drop in the direction of the incident wave's Poynting vector. It should be noted that this formulation is valid for other types of scatterers having orthogonal planes of symmetry (van de Hulst 1981) (ellipsoids and circular cylinders, for example) regardless of size relative to the wavelength.

a. Optimal polarizations for canted particle

Rewriting the principal plane scattering matrix for a single drop (4) in the normalized form yields

$$\mathbf{S}^0 = \begin{bmatrix} 1 & 0 \\ 0 & a^0 e^{i\delta^0} \end{bmatrix}, \quad (9)$$

where $a^0 \equiv |S^0_{VV}|/|S^0_{HH}|$. The phase δ^0 is the phase difference between the vertical and horizontally polarized signals when the drop is in its principal orientation. The Graves matrix can be found for an arbitrary canting angle from $\mathbf{S}^0$ as

$$\mathbf{G} = \mathbf{S}^\dagger\mathbf{S} = (\mathbf{R}^{-1}\mathbf{S}^0\mathbf{R})^\dagger\mathbf{R}^{-1}\mathbf{S}^0\mathbf{R}$$
$$= \mathbf{R}^{-1}\mathbf{S}^{0\dagger}\mathbf{S}^0\mathbf{R} = \mathbf{R}^{-1}\mathbf{G}^0\mathbf{R}.$$

Thus, the Graves matrix for an arbitrary canted particle can be written in terms of the Graves matrix obtained from the principal plane scattering matrix $\mathbf{S}^0$ and the rotation matrix $\mathbf{R}$. The Graves matrix $\mathbf{G}^0$ can be expressed in terms of the elements of $\mathbf{S}^0$ in (9), is also a diagonal matrix, and reduces to

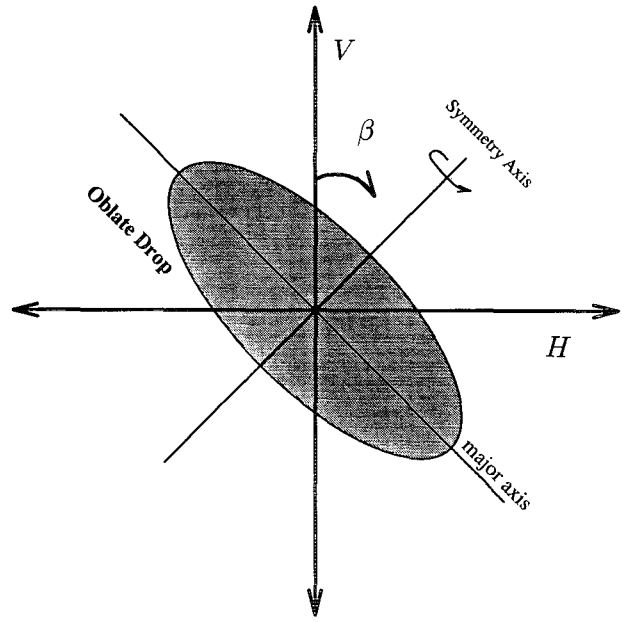

FIG. 1. Single oblate drop canted in the plane of polarization. The canting angle β is defined clockwise from the local vertical. The incident wave is propagating into the page.

$$\mathbb{G}^0 = \begin{bmatrix} 1 & 0 \\ 0 & (a^0)^2 \end{bmatrix}. \quad (10)$$

The principal plane matrix $\mathbb{G}^0$ is independent of the phase δ^0, and therefore, $\mathbb{G}$ and the optimal polarizations are independent of the phase as well. Since $\mathbb{G}$ is obtained from an orthogonal transformation on $\mathbb{G}^0$, the eigenvalues of $\mathbb{G}$ are simply 1 and $(a^0)^2$ (e.g., Strang 1988, 304).

The asymmetry ratio defined as the ratio of $\mathbb{G}$ eigenvalues is

$$\mathcal{A} = \frac{1}{(a^0)^2}. \quad (11)$$

The eigenvectors associated with the maximal and minimal eigenvalues are found to be

$$\mathbb{E}_1 = \frac{1}{(1+\tan^2\beta)^{1/2}}\begin{bmatrix} 1 \\ \tan\beta \end{bmatrix};$$

$$\mathbb{E}_2 = \frac{1}{(1+\cot^2\beta)^{1/2}}\begin{bmatrix} 1 \\ \cot\beta \end{bmatrix}. \quad (12)$$

A recipe for calculating eigenvectors can be found in linear algebra texts (e.g., Strang 1988, p. 246). The corresponding tilts and ellipticities are given by (see appendix B for details)

$$\tau_1 = -\beta \quad (13)$$

$$\tau_2 = 90° - \beta \quad (14)$$

$$\epsilon_1 = \epsilon_2 = 0. \quad (15)$$

Since the ellipticity is zero, the polarizations that maximize or minimize the scattered energy are always *linear* regardless of the differential backscatter phase δ^0. This is a somewhat counterintuitive result.[3] The two tilts depend only on the canting angle β and are orthogonal as expected.

As was anticipated, the optimal tilt and ellipticity are independent of particle size and shape. The asymmetry ratio, however, is a function of particle size and shape and is independent of orientation. For Rayleigh particles, a^0 is proportional to the axial ratio of the drop and is independent of size. When the particle is large, however, a^0 no longer has a simple dependence on the drop shape.

In summary, these results show that for any single scatterer fulfilling the symmetry condition for a principal plane scattering matrix, the effects of orientation size, and shape are separated using this approach. These results hold for particle sizes in the Rayleigh as well as in the Mie regions. Next, the optimal polarizations for an oblate spheroid are studied since this particle shape is the basis of our ensemble calculations later in the paper.

[3] This result is reminiscent of the helicity argument–symmetry condition given in Huynen (1978, p. 659).

b. *Optimal polarizations for oblate spheroid at S band*

Oblate spheroids are used here to model raindrops with equilibrium shapes. Although drops having cusps (Pruppacher-and-Pitter drops; Pruppacher and Beard 1970) have been used in models in the past (e.g., Oguchi 1977), for this study oblate spheroidal equilibrium shapes are sufficient.

In the principal plane scattering matrix $\mathbf{S}^0$ (9), a^0 will be less than unity since the horizontal axis of the drop is larger than the vertical. Calculations show that a^0 remains below unity even for the largest drops considered in this study. The differential backscatter phase difference δ^0 is negligible for drops even as large as 6 mm at S band and is ignored in the rest of this work. The asymmetry ratio (11) becomes, using the definition of a^0 in (9),

$$\mathcal{A} = \frac{1}{(a^0)^2} = \left(\frac{|S^0_{HH}|}{|S^0_{VV}|}\right)^2. \tag{16}$$

Thus, the asymmetry ratio $\mathcal{A}$ is simply the ratio of the squared magnitudes from the horizontal and vertical principal plane returns analogous to Z_{DR} [the ratio of the $|S_{HH}|^2$ and $|S_{VV}|^2$ elements of $\mathbf{S}$ in (5)]. Unlike Z_{DR}, however, $\mathcal{A}$ is independent of the canting angle β (a mathematical property of eigenvalues). The re-

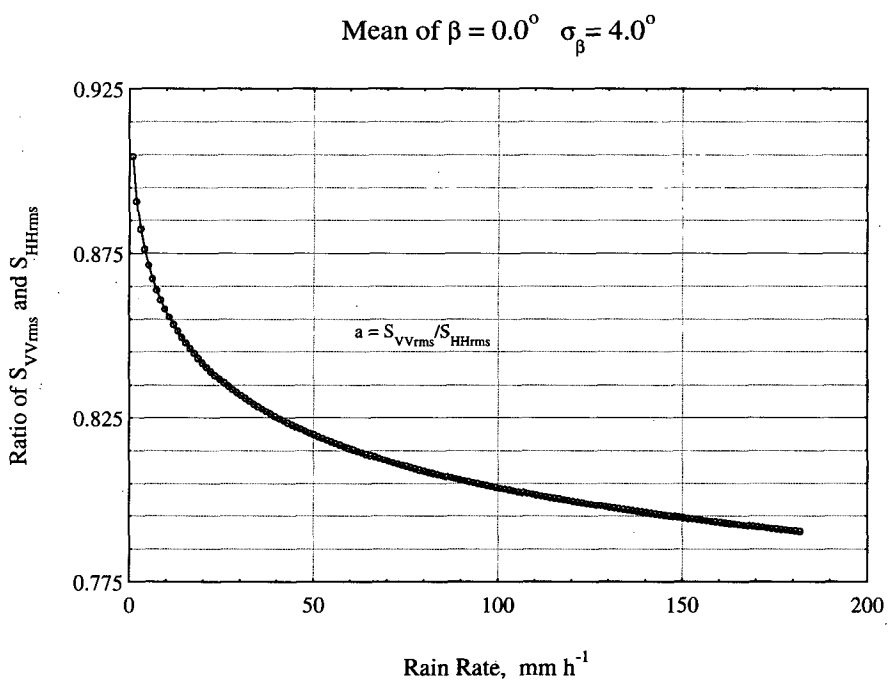

FIG. 2. The ratio of $S_{VV\text{rms}}$ and $S_{HH\text{rms}}$ matrix elements, a versus the rain rate R (mm h^{-1}). The frequency of the incident wave is 2.80 GHz (λ = 10.7 cm) and the index of refraction is assumed that of water at a temperature of T = 0.0°C (Ray 1972). Note that for low rain rates, when most drops are small and spherical, the ratio tends toward unity.

lationship between the asymmetry ratio and differential reflectivity is discussed in more detail in a later section.

The eigenvector that corresponds to the maximum scattered power is labeled as E_{op} and is given as

$$E_{op} = \frac{1}{(1 + \tan^2\beta)^{1/2}} \begin{bmatrix} 1 \\ \tan\beta \end{bmatrix}. \quad (17)$$

The corresponding optimal tilt and optimal ellipticity are

$$\tau_{op} = -\beta \quad (18)$$

$$\epsilon_{op} = 0. \quad (19)$$

That is, the optimal tilt is identical to the canting angle. (The minus sign results because the canting angle is defined from the local vertical and tilt is defined from the local horizontal; see Fig. 1.)

In the single-scatterer case, the optimal tilt is similar to the canting parameter

$$\gamma_\beta = \frac{|S_{HV}|^2}{|S_{VV} - S_{HH}|^2} = \cos^2(\beta)\sin^2(\beta) \quad (20)$$

proposed in Jameson (1985a). The subscript β is used to distinguish between canting in a plane and true canting (not constrained to a plane) that was used in Jameson (1985a). This parameter depends only on β, in the single drop case and, therefore, must be related to optimal tilt. In fact, for small β, $\gamma^{1/2}$ reduces to τ_{op}. A comparison between the two parameters is made in a later section when an ensemble of drops is considered.

4. Ensemble of hydrometeors

While a single drop is easier to interpret, natural rain consists of a distribution of drops of various sizes and shapes, and the previous analysis must be extended to an ensemble of raindrops. Using the principal plane scattering amplitudes calculated by the T-matrix method, the scattering matrix of an ensemble of drops is computed following the model introduced in Jameson (1985a, 1986). Only a brief description is given here, and the reader is referred to that paper for details.

The model used in Jameson (1985a, 1986) includes three-dimensional canting and nonzero radar elevation angles, and parameterizes the effects of drop oscillations. Here the model is simplified in an attempt to obtain a better understanding of the basic physics of the polarization parameters relationships to hydrometeor characteristics. The key assumptions in our simplified model are as follows.

- The drops are modeled as equilibrium-shaped oblate spheroids. The effects of drop oscillations are not included.[4]
- The drops are constrained to cant only in the plane of polarization. The radar elevation angle is zero.
- The canting angle distribution is assumed Gaussian with mean canting angle $\bar{\beta}$ and standard deviation σ_β.

The principal plane scattering matrices are modified by average values of geometric coefficients to yield the average scattering matrix for an ensemble of raindrops. The simulated scattering matrices are then used to calculate the polarization parameters $\mathcal{A}$, ϵ_{op}, and τ_{op} versus mean axial ratio (through the rain rate) with $\bar{\beta}$ and σ_β as parameters.

a. Details of calculations

The computations of the principal plane complex scattering amplitudes for both H and V polarizations are carried out using the T-matrix method (e.g., Waterman 1965, 1971; Warner and Hizal 1976; Barber and Hill 1990) for oblate spheroids. The axial ratios used are those of equilibrium shaped drops; that is, the axial ratio is a linear function of the equal-volume drop diameter D (e.g., Pruppacher and Beard 1970; Oguchi 1977):

$$r(D) = 1.03 - 0.62D, \quad D \geq 0.1 \text{ cm}. \quad (21)$$

Drop diameters range from 0.01 to 0.6 cm. The frequency of the incident wave is 2.80 GHz (λ = 10.7 cm), and the index of refraction is assumed that of water at a temperature of $T = 0.0°$C (Ray 1972). Both the backward and forward complex scattering amplitudes (magnitude and phase) are calculated over the range of drop diameters specified. For this wavelength, the backscatter differential phase shift δ can be neglected and is not considered in further calculations. The drop size distribution used in this model is of the form

$$N(D)dD = N_0 e^{-\Delta D} dD, \quad (22)$$

where $N_0 = 0.07R^{0.37}$ cm^{-4} and $\Delta = 38R^{-0.14}$ cm^{-1}. These values have been used to characterize thunderstorms (Sekhon and Srivastava 1971). The rain rate R is expressed in millimeters per hour and, for this study, ranges from 1 to 180 mm h^{-1}. Since this drop size distribution is exponential, the smallest drops occur much more frequently than the larger ones. It is these larger drops with axial ratios deviating most strongly from unity, however, that determine the polarization characteristics of the precipitation.

The magnitudes of the scattering amplitudes are calculated for three elements of the scattering matrix (the matrix is assumed symmetric). Since most radars measure power, the magnitudes are calculated in an rms sense; that is, each squared magnitude is weighted by both the average values of the canting angle distribution and the drop size distribution. The weighted squared magnitudes are then added and normalized to

[4] Calculations parameterizing the effects of drop oscillations show that at the heaviest rain rate the magnitudes and phases of the scattering matrix elements differed less than 1% when compared with the simplified model used here. Consequently, the results given here may apply to a less restricted and more realistic ensemble of drops.

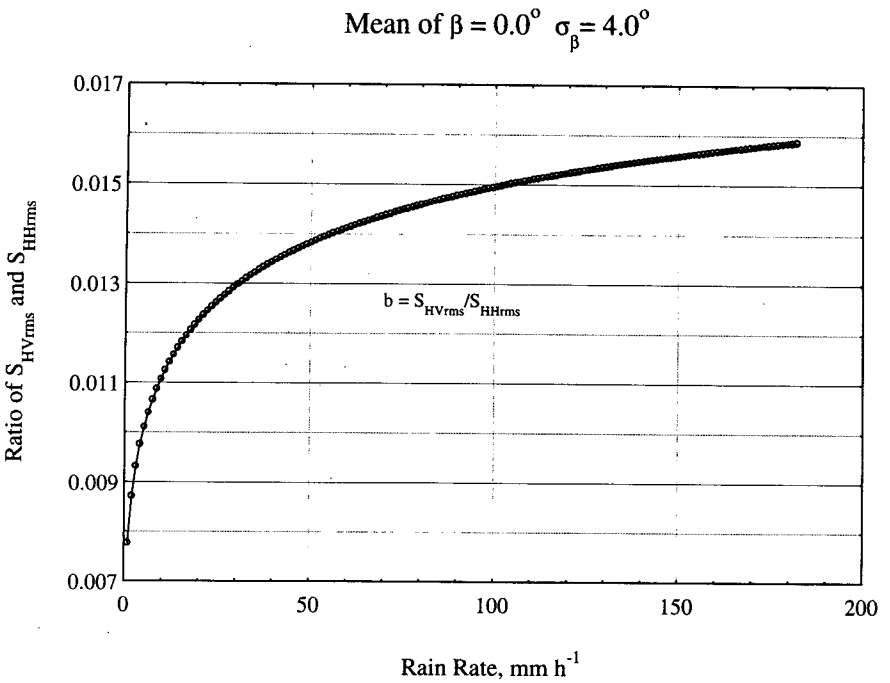

FIG. 3. The ratio of $S_{HV\text{rms}}$ and $S_{HH\text{rms}}$ matrix elements b is shown versus the rain rate R (mm h^{-1}). The frequency of the incident wave is 2.80 GHz (λ = 10.7 cm) and the index of refraction is assumed that of water at a temperature of T = 0.0°C (Ray, 1972). Note that for low rain rates when most drops are spherical, the ratio approaches zero because there are fewer canted oblate drops to produce a cross-polarized component in the scattered wave.

obtain the average rms amplitudes of the scattering matrix. These real quantities are denoted as $S_{HH\text{rms}}$, $S_{VV\text{rms}}$, and $S_{HV\text{rms}}$. Note that all averaging is performed over drops, and therefore, the rms values should be interpreted as resulting from spatial averaging. Assuming ergodicity, these rms amplitudes are equivalent to time averages. Such an averaging scheme was examined in Schroth et al. (1988; see, in particular, p. 811 describing the *average relative* **S** *matrix*) for use with the DLR radar. We note, in passing, that no assumptions on correlations between matrix elements are made. Rates of propagation phase shift are computed for the copolarized elements from the forward-scattering amplitudes of each drop weighted by the drop size distribution (e.g., Aydin and Zhao 1990). The model scattering matrix for the ensemble is therefore

$$\mathbf{S}_{\text{rms}} = \begin{bmatrix} 1 & be^{i\phi/2} \\ be^{i\phi/2} & ae^{i(\phi)} \end{bmatrix}, \qquad (23)$$

where a and b are now rms magnitudes equal to $S_{VV\text{rms}}/S_{HH\text{rms}}$ and $S_{HV\text{rms}}/S_{HH\text{rms}}$, respectively (Schroth et al. 1988). Since the magnitudes of the elements are rms values, the matrix is denoted as $\mathbf{S}_{\text{rms}}$. We stress that the sign information about the canting angle is lost. Therefore, we give ϵ_{op} and τ_{op} the labels *apparent* optimal ellipticity and tilt in the ensemble case. The measurement of these rms quantities is discussed in section 4d.

Plots of the calculated rms matrix elements versus rain rate are presented in Figs. 2 and 3 for a canting distribution with mean $\bar{\beta} = 0.0°$ and $\sigma_\beta = 4.0°$ (Beard and Jameson 1983). Figure 2 shows the value of a (proportional to Z_{DR}) over the entire range of rain rates. The curve tends toward unity at small rain rates because the majority of drops are spherical. At larger rain rates, more of the drops are oblate and a deviates from unity. In Fig. 3, the off-diagonal term b (proportional to LDR) is plotted as a function of rain rate. Here b is small at low rain rates since no cross-polarized returns are expected from spherical drops. As the rain rate increases, so does the number of large oblate drops, some of which are canted and cause a cross-polarized echo. The rate of propagation differential phase shift is presented in Fig. 4. Note that Φ is a rate in degrees per kilometer. Since Φ is defined as $VV - HH$, this becomes more negative with increasing rain rate.

b. Neglecting propagation phase

In this section propagation phase effects are ignored entirely in order to gain insight into the dependence of the optimal polarizations on the canting angle distribution. The phase ϕ in (23) is set to zero, and we regard the measurement as being made in the first rain gate. Note that in the absence of propagation phase $\mathbf{S}_{\text{rms}}$ is real and requires only the measurement of the

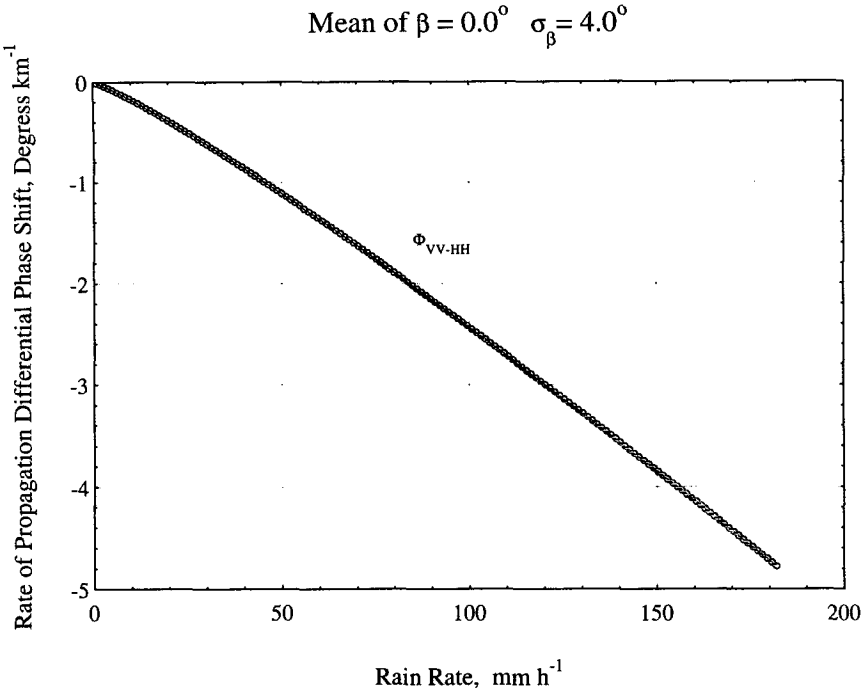

FIG. 4. Rate of propagation differential phase shift Φ versus rain rate (mm h^{-1}). The frequency of the incident wave is 2.80 GHz (λ = 10.7 cm) and the index of refraction is assumed that of water at a temperature of T = 0.0°C (Ray 1972). Note that Φ is presented as a rate with units of degrees per kilometer. Also note that Φ is defined as $\Phi_{VV} - \Phi_{HH}$ because **S** is normalized by S_{HH}.

three rms magnitudes. Using the simulated scattering matrices for the range of rain rates mentioned above, the polarization parameters $\mathcal{A}$, ϵ_{op}, and τ_{op} can be calculated.

1) ASYMMETRY RATIO AND Z_{DR}

Given the fact that the asymmetry ratio (in decibels) in the absence of canting is equivalent to the differential reflectivity, it is natural to compare the two. The asymmetry ratio and Z_{DR} are calculated as functions of the rain rate and the canting angle parameters. Since equilibrium shapes are used, the rain rate R depends on the mean drop size and shape through the drop size distribution. The mean axial ratio is of physical importance, and since radars measure reflectivity, we examine the dependence of $\mathcal{A}$ on the reflectivity-weighted mean axial ratio $\mathcal{R}$ (e.g., Jameson 1983). This is defined as

$$\mathcal{R} = \frac{\int r(D)\,|S^0_{HH}(D)|^2 N(D)\,dD}{\int |S^0_{HH}(D)|^2 N(D)\,dD}.$$

Figure 5 shows the asymmetry ratio (dB) plotted versus $\mathcal{R}$ (dB). The canting angle parameters have been fixed at $\bar{\beta} = 0°$ and $\sigma_\beta = 4.0°$. There exists an almost linear relationship between the two on a log scale. This leads to a power-law relationship of the form $\mathcal{A} = \mathcal{R}^x$, with $x = -2.28$ as shown in Fig. 5 (for the 4° standard deviation of canting angles typical of rain). Comparison of $\mathcal{A}$ with Z_{DR} (Fig. 5) shows that the asymmetry ratio seems to contain the same information about the mean shape as does Z_{DR} (at least in rain when standard deviations of canting angles are small). The differential reflectivity is, however, more sensitive to the canting angle distribution than is $\mathcal{A}$, as illustrated in Figs. 6 and 7.

The dependence of $\mathcal{A}$ and Z_{DR} on the mean canting angle $\bar{\beta}$ is shown in Fig. 6 for two rain rates of 6.4 and 29.1 mm h^{-1}. The standard deviation σ_β is held constant at 4°. Values of $\bar{\beta}$ have been chosen to vary from 0° to 10°. The values of $\bar{\beta}$ are extended beyond the physically plausible range for rain but could occur in wet hail, etc. As expected, Z_{DR} decreases with increasing $\bar{\beta}$ since the returns due to canted drops have a cross-polarized component. The asymmetry ratio $\mathcal{A}$ is practically constant for $\bar{\beta} \leq 4°$ and then increases slightly. As in a single drop case, changing $\bar{\beta}$ does not appear to affect $\mathcal{A}$ greatly. While the reason for the small gradual increase requires further investigation, it is evident that changes in β affect $\mathcal{A}$ only slightly.

The dependence of the $\mathcal{A}$ and Z_{DR} on the standard deviation of the canting angle σ_β is shown in Fig. 7 for the same two rain rates as in Fig. 6. Values of σ_β as

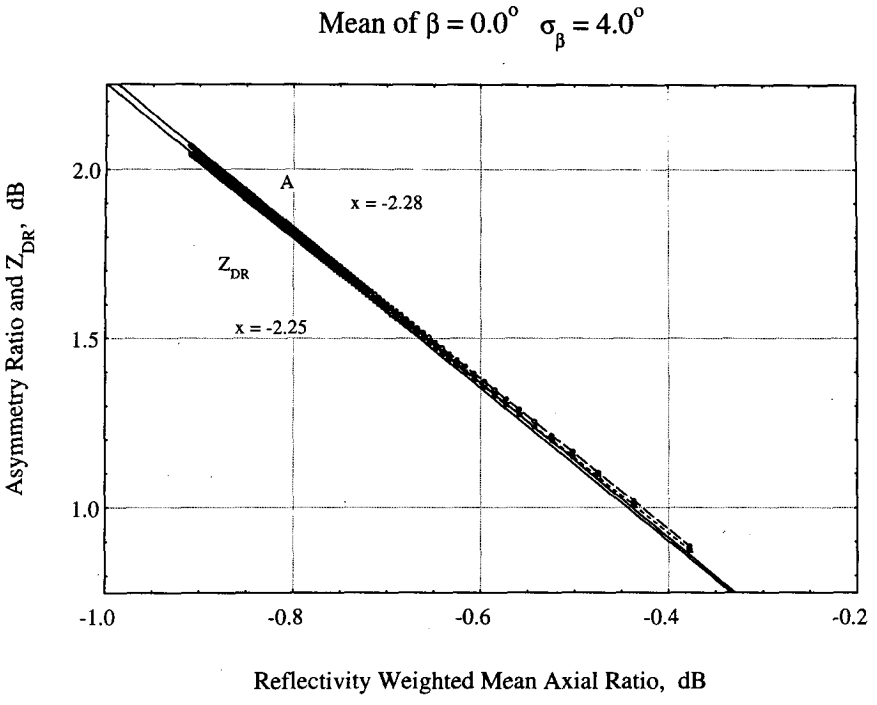

FIG. 5. The asymmetry ratio $\mathcal{A}$ (dB) and Z_{DR} versus the reflectivity-weighted mean axial ratio $\mathcal{A}$ (dB). Both curves are shown along with their power-law fits ($y = \mathcal{R}^x$).

high as 30° do not normally occur in rain but might be typical of other forms of precipitation. Setting the mean canting angle to zero, the asymmetry ratio $\mathcal{A}$ at a constant rain rate increases slightly as σ_β increases. This is in contrast with Z_{DR}, which decreases sharply as σ_β increases. These results are similar to the dependence of $\mathcal{A}$ and Z_{DR} on the mean canting angle. Again, the mechanism responsible for the slight increase of $\mathcal{A}$ with σ_β is not clear. We suspect that this might be an artifact caused by the loss of canting angle sign information in the rms model.

2) APPARENT OPTIMAL ELLIPTICITY AND TILT

Next we examine the relationships between ϵ_{op} and τ_{op} and the three microphysical parameters $\mathcal{R}$, $\bar{\beta}$, and σ_β. In this section, the effects of the rms scattering matrix are more apparent. Indeed, in spite of the fact that drops cant in both positive and negative directions, the sign information is lost in the process of computing the rms scattering matrix. As a result, the optimal polarization tilts are always positive and must, therefore, also be interpreted in the rms sense.

As expected from the single drop case, the apparent optimal tilt and ellipticity are fairly insensitive to $\mathcal{R}$ and therefore rain rate (they vary by less than 1°). Consequently, the ϵ_{op} and τ_{op} versus **R** plots are not included. However, this insensitivity is illustrated for the tilt in Figs. 8 and 9 where rain rate is used as a parameter.

Figure 8 is a plot of τ_{op} versus $\bar{\beta}$ for four rain rates (6.4, 29.1, 58.5, 94.6 mm h^{-1}). Note that for small $\bar{\beta}$, the tilt does not approach zero and is, in fact, slightly larger than σ_β. This fact must be interpreted in the rms sense (see also section 4d); that is, all drops are canted in a positive direction with an effective average angle slightly larger than σ_β. At larger angles, the behavior of the apparent (rms) optimal tilt shows an almost linear dependence for large mean canting angles ($\bar{\beta} \geq 4°$). This is reminiscent of the single drop case. One interesting feature of this graph is the insensitivity of the apparent optimal tilt to the rain rate. This suggests that it can be used as a measure of mean canting at least in the absence of any propagation phase shift.

The dependence of the apparent optimal tilt τ_{op} on σ_β is shown in Fig. 9. The standard deviation of the canting angle distribution is plotted versus the tilt at the same four rain rates as in Fig. 8. The mean canting angle in this case is zero. As expected, $\tau_{op} \to 0$ as $\sigma_\beta \to 0$, since in that case all drops have a canting angle of $\beta = 0°$. The tilt has an almost linear dependence on the standard deviation for small $\bar{\beta}$ at all rain rates. The linear depolarization ratio [LDR = 10 log(b^2)] is plotted along with τ_{op}. The canting parameter γ_β (introduced in Jameson 1985a), which is a function of the canting distribution only, is also plotted for comparison. The optimal tilt appears to be the variable of choice to use as an estimate of σ_β. Another interesting feature of Fig. 9 is the apparent tilt's insensitivity to $\mathcal{R}$ and thus rain

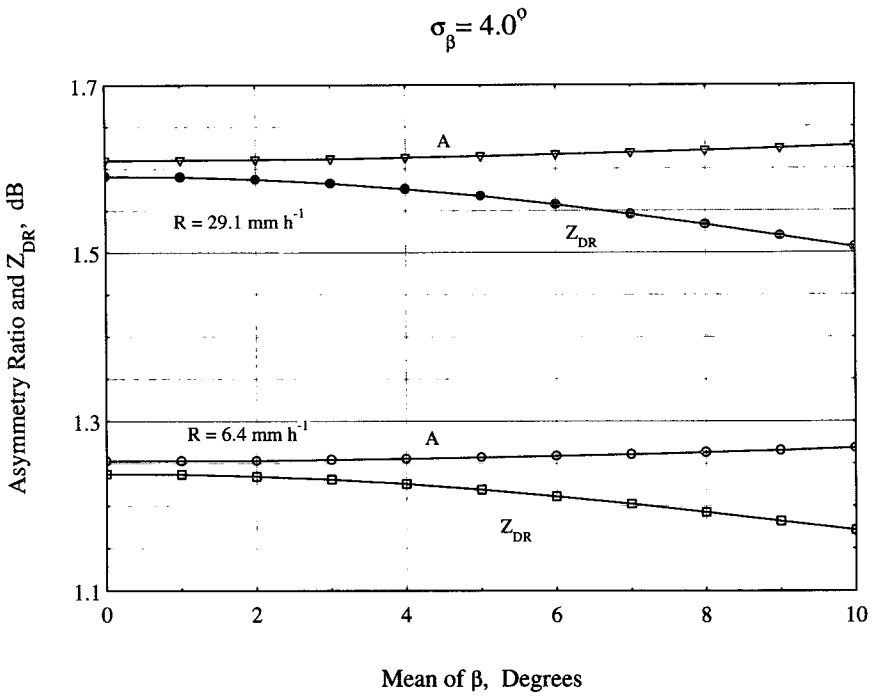

FIG. 6. The asymmetry ratio $\mathcal{A}$ (dB) and Z_{DR} versus mean canting angle $\bar{\beta}$ for two rain rates of 6.4 and 29.1 mm h^{-1}. The standard deviation of canting angles σ_β has been set at 4°. In each case, $\mathcal{A}$ remains fairly constant while Z_{DR} decreases.

rate. This seems to suggest a measurement of σ_β directly from τ_{op} when the propagation differential phase shift and $\bar{\beta}$ are small.

The apparent ellipticity ϵ_{op} (not shown) is not a function of either $\bar{\beta}$ or σ_β in the absence of propagation differential phase shift. In fact, since **S** consists of only real quantities in this case, the apparent optimal ellipticity is identically zero. Hence, plots of ϵ_{op} are not shown.

In summary, the asymmetry ratio $\mathcal{A}$ has a power-law-type relationship with the reflectivity-weighted mean axial ratio. The asymmetry ratio gives a slight improvement over Z_{DR} as a measure of $\mathcal{R}$ and is less affected by particle canting, particularly when σ_β is large. The asymmetry ratio does, however, require the additional measurement of the cross-polarized power. In fact, an expression for $\mathcal{A}$ has been derived in terms of the rms amplitudes and is given in appendix C.

The apparent optimal tilt is a function of both the mean canting angle $\bar{\beta}$ and the standard deviation of the canting angle σ_β. Since the mean canting angles of hydrometeors are typically close to zero (e.g., Jameson 1985a), however, the apparent optimal tilt can be used to measure σ_β. The apparent optimal ellipticity on the other hand has a rather striking insensitivity to both $\bar{\beta}$ and σ_β when ϕ is negligible. In the next section it is shown that propagation phase affects both the apparent optimal ellipticity and tilt.

c. *Including propagation effects*

In order to analyze backscattering from range gates farther into the medium one has to consider the incident wave traversing through a distance $2L$ containing rain (L is the one-way propagation distance in kilometers). For the purposes of this propagation study, we assume the mean canting angle of the precipitation to be zero and concentrate on the variance of the distribution. The dependence of the apparent optimal tilt and ellipticity on σ_β, in the presence of propagation phase, is discussed next.

Calculations have been performed for L = 8 km (the total propagation distance is $2L$). The propagation differential phase shift $\phi = 2L\Phi$, where Φ is the rate of propagation differential phase shift. The resulting rms scattering matrices have been used to calculate the polarization parameters $\mathcal{A}$, τ_{op}, and ϵ_{op}. The asymmetry ratio $\mathcal{A}$ is not affected by propagation effects; that is, it is not a function of propagation distance L and will not be considered any further in this section (see appendix C).

The response of τ_{op} to canting shows a greater dependence on rain rate when including propagation effects, because the specific propagation differential phase shift Φ is highly dependent on rain rate (see Fig. 4). This dependence of Φ on R is amplified in the scattering matrix by the 8-km total pathlength. (Our model includes the two-way propagation distance but results

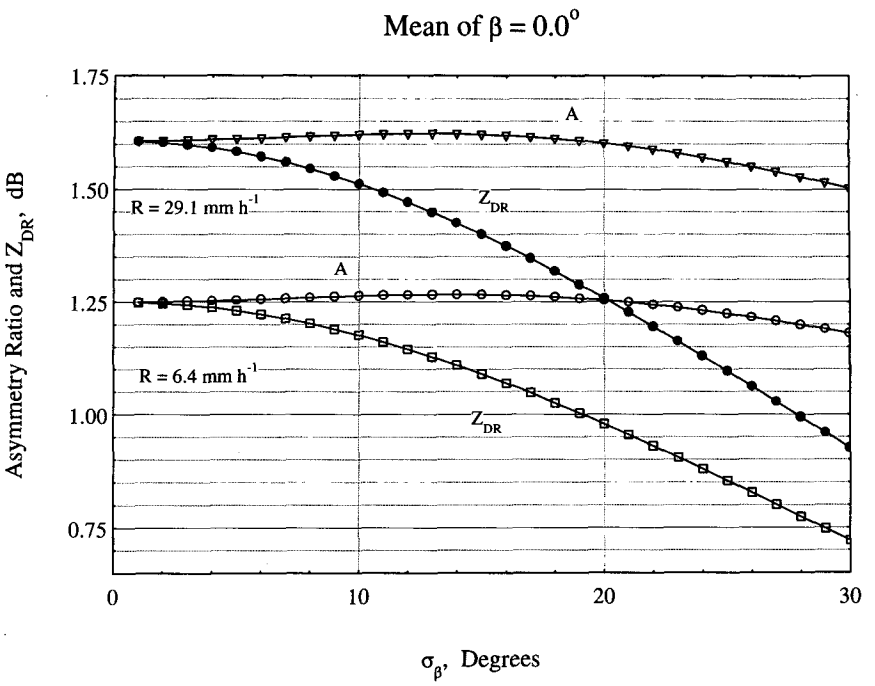

FIG. 7. The asymmetry ratio $\mathcal{A}$ (dB) and Z_{DR} versus the standard deviation of the canting angle distribution σ_β for the same two rain rates as in Fig. 6. The propagation phase shift has been set to zero and $\sigma_\beta = 4°$. Again, Z_{DR} decreases rapidly while $\mathcal{A}$ is less affected by σ_β.

are in terms of L the one-way propagation distance.) Figure 10 shows τ_{op} versus σ_β when including propagation effects for four rain rates. The propagation differential phase has the effect of spreading out the curves when compared with Fig. 9. If the propagation phase effects could be removed by measuring the propagation phase independently, however, τ_{op} could still be used to determine canting parameters. Note that curves for LDR and γ_β are not present in Fig. 10, since by definition both are independent of propagation differential phase shift.

In the absence of propagation phase, the ellipticity is not a function of the canting parameters [see section 4b(2)]. When propagation phase is present, however, the ellipticity is a measurable function of both $\bar{\beta}$ and σ_β. For example, a plot of the apparent optimal ellipticity versus σ_β is shown in Fig. 11 for the same four rain rates as in Fig. 10. The apparent optimal ellipticity now depends on rain rate for the same reason as tilt, namely, the fact that the specific propagation differential phase shift is a function of rain rate. For high rain rates and large σ_β, ϵ_{op} can be several degrees. This, however, may not be large enough for practical measurements [although differential phase measurements of 1° or less have been reported (Doviak and Zrnić 1993)].

We next examine the dependence of the optimal polarizations on the one-way propagation distance L and, thus, the propagation differential phase shift ϕ. Scattering matrices (23) are computed for a constant rain rate but for a range of propagation distances. The apparent optimal tilt and ellipticity are then determined from each matrix. Figure 12 shows the dependence of the apparent tilt and ellipticity on the one-way propagation path L for a distance out to 100 km for a rain rate of 94.6 mm h^{-1}. Of course, one is unlikely to ever encounter a one-way propagation path of 100 km in 94.6 mm h^{-1} rain. Nevertheless, the propagation path is extended to this exaggerated value simply to illustrate the periodic dependence of ϵ_{op} and τ_{op} on L. The canting angle parameters are set at $\bar{\beta} = 0°$ and $\sigma_\beta = 4°$. The dependence of both ellipticity and tilt on L appear surprisingly sinusoidal. In retrospect, this cyclic behavior should be anticipated as ϕ rotates through 360° over sufficiently long propagation distances. It is interesting to note that the amplitudes of the τ_{op} and ϵ_{op} curves are the same (approximately 4.5°) while they differ in phase by about 40 km. This functional dependence prompted us to examine the relationship of ellipticity and tilt to the propagation differential phase more closely. As shown in the previous section, the apparent ellipticity is independent of the canting parameters, while the apparent tilt does depend on the canting distribution. In an attempt to find an optimal polarization parameter that will provide us with a measure of propagation phase, we concentrate on the apparent optimal ellipticity because it is not a measurable function of canting in the absence of propagation phase.

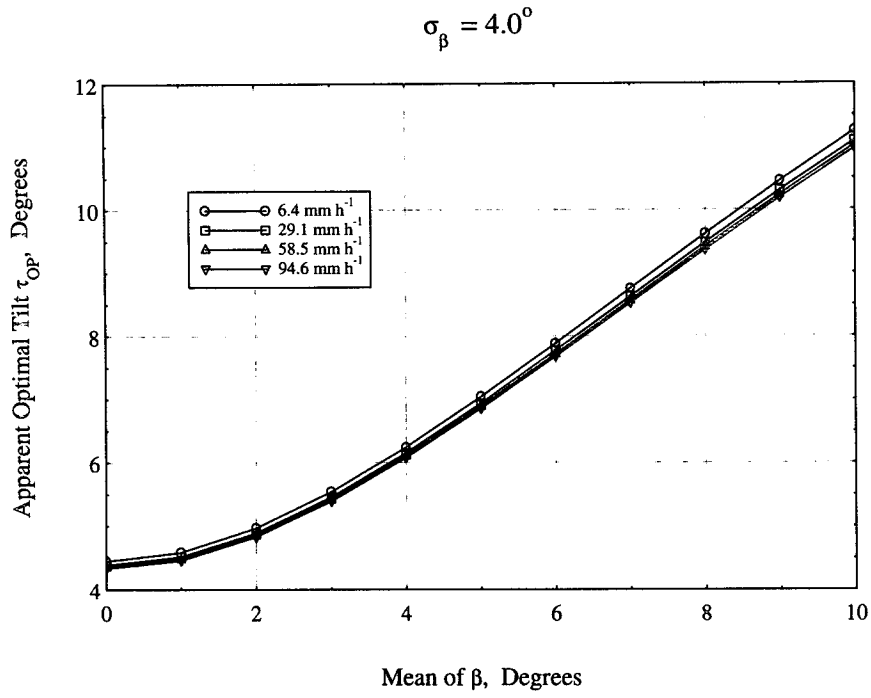

FIG. 8. The apparent optimal tilt τ_{op} versus the mean canting angle $\bar{\beta}$ for four rain rates (6.4, 29.1, 58.5, 94.6 mm h^{-1}). The propagation phase shift has been set to zero and $\sigma_\beta = 4°$. The behavior of the apparent optimal tilt shows an almost linear dependence for large mean canting angles ($\bar{\beta} \geq 4°$). One interesting feature of this graph is the insensitivity of the apparent optimal tilt to the rain rate. Note that for small $\bar{\beta}$ the tilt does not approach zero and is, in fact, slightly larger than σ_β. This occurs because of the rms artifacts present whenever the standard deviation of the canting angles is not zero.

A sinusoidal-type dependence of the apparent optimal ellipticity on the propagation differential phase suggests a simple dependence on the matrix elements of $\mathbf{S}_{rms}$ (23). To explore this dependence, we have used a symbolic manipulator (Macsyma) to determine algebraically the dependence of ϵ_{op} on all the elements of the scattering matrix; that is, $\epsilon_{op} = \epsilon_{op}(a, b, \phi)$. The amplitude of ϵ_{op} oscillations appear to be a function only of the magnitudes a and b, while the lag of the ϵ_{op} curve depends only on the propagation differential phase shift ϕ. Since ϕ can be expressed as $\phi = 2L\Phi$, where Φ is the rate of propagation differential phase shift in degrees per kilometer, the period of the sine wave depends on Φ. The steps in obtaining ϵ_{op} as a function of a, b, and ϕ along with the explicit expression for ϵ_{op} are given in appendix C. In typical experiments, ϵ_{op} would probably not be detectable until its magnitude is larger than about 1°. At a rain rate of 94.6 mm h^{-1}, this does not happen until the propagation distance exceeds 3 km.

In summary, the study of the optimal polarization parameters dependence on the characteristics of the precipitation including the canting angle distribution and propagation effects leads to the following conclusions. The asymmetry ratio $\mathcal{A}$ is a function of the reflectivity-weighted mean axial ratio $\mathcal{R}$ and therefore a function of rain rate, but it is less sensitive to canting than Z_{DR}. Furthermore, $\mathcal{A}$ is independent of the propagation phase. Thus, the asymmetry ratio can be regarded as a generalization of Z_{DR} (at least for S band) because it is a combination of Z_{DR} and LDR and it reduces to Z_{DR} in the no-canting limit.

The apparent optimal polarization parameters τ_{op} and ϵ_{op} are both functions of the canting distribution parameters and the propagation phase; however, both are weak functions of the rain rate and $\mathcal{R}$. The relationships are simplified considerably, however, in the case of zero mean canting angle. It is therefore possible to envision estimating σ_β and ϕ based on measurements of τ_{op} and ϵ_{op}. In the previous sections, the behavior of the optimal polarization parameters has been examined while holding σ_β or ϕ fixed. The functional relationships between these variables can be rather complex, but when combined with other quantities τ_{op} and ϵ_{op} might prove to be of practical use. If it is assumed that the mean canting angle of hydrometeors is close to zero, then τ_{op} and ϵ_{op} depend only on σ_β and the phase ϕ. In principle, it should be possible to estimate both σ_β and the propagation phase ϕ using τ_{op} and ϵ_{op} if these latter two quantities

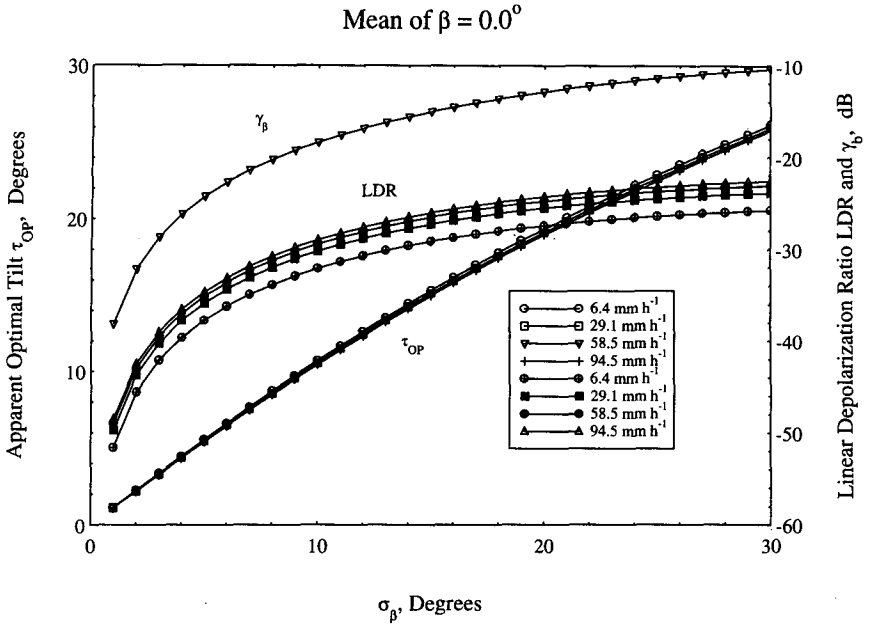

FIG. 9. The apparent optimal tilt τ_{op} versus the standard deviation of the canting angle distribution σ_β for the same four rain rates as in Fig. 8. Note the two y axes needed to put all three curves on the same plot. The propagation phase shift has been set to zero and $\bar{\beta} = 0°$. The tilt (using the left y axis) has an almost linear dependence on the standard deviation for all rain rates. One observes that the apparent optimal tilt is nearly independent of rain rate. The LDR and γ_β have also been plotted on this graph (using the right y axis). Note that LDR varies considerably with rain rate and γ_β depends only on the canting distribution.

can be readily measured from the rms matrix elements.

d. On a possible measurement scheme

Obviously, any new variable is most useful if it can be measured. Here we give examples of measurement schemes that will allow the determination of $\mathcal{A}$, ϵ_{op}, and τ_{op} from real radar data. In order to measure these parameters, one needs either the average rms (see also Schroth et al. 1988) or the instantaneous full scattering matrix. While the former is easier to measure (and is our focus here), the latter contains more information. As demonstrated in this paper, the rms scattering matrix calculated from the average powers at horizontal and vertical copolarizations and the average power at cross-polarization can be used to obtain $\mathcal{A}$, ϵ_{op}, and τ_{op} in the absence of propagation effects. Such rms measurements are possible on several research radars today operating at S band and would provide the microphysical information discussed above. In fact, such a scheme was proposed in Schroth et al. (1988) but for C band where backscatter differential phase and attenuation effects are not negligible. It should be noted, however, that these three measurements are sufficient to calculate only the rms values of the optimal polarization parameters because of the loss of sign information as discussed in section 4a.[5] This provides motivation to look at an instantaneous measurement of **S** that will be a subject of a future publication. For now, we will confine ourselves to brief remarks.

Assume that a radar is capable of measuring the full scattering matrix (amplitudes and phases) either by switching the transmitted polarization states well below the decorrelation time of the precipitation or by obtaining an instantaneous scattering matrix with interpolation (e.g., Chandrasekar et al. 1993). Furthermore, envision a time series of these matrices measured for a given range and elevation angle, that is, $\mathbf{S}_1, \mathbf{S}_2, \ldots, \mathbf{S}_N$. For each $\mathbf{S}_i$, the three polarization parameters $\mathcal{A}_i$, ϵ_{opi}, and τ_{opi} can be calculated. These calculations involve the solution of a simple 2×2 eigenvalue problem; in particular, the asymmetry ratio can be obtained simply from a quadratic equation involving the elements of **G**. The ellipticity and tilt are calculated from the eigenvectors using inverse trigonometric functions.

The calculations result in a fluctuating time series for each polarization parameter. For example, the optimal tilt will fluctuate in time giving positive and negative values. The mean value of τ_{op} should be zero on

[5] Also note that the interpretation of the rms scattering matrix as an operator acting on some polarization vector is no longer clear.

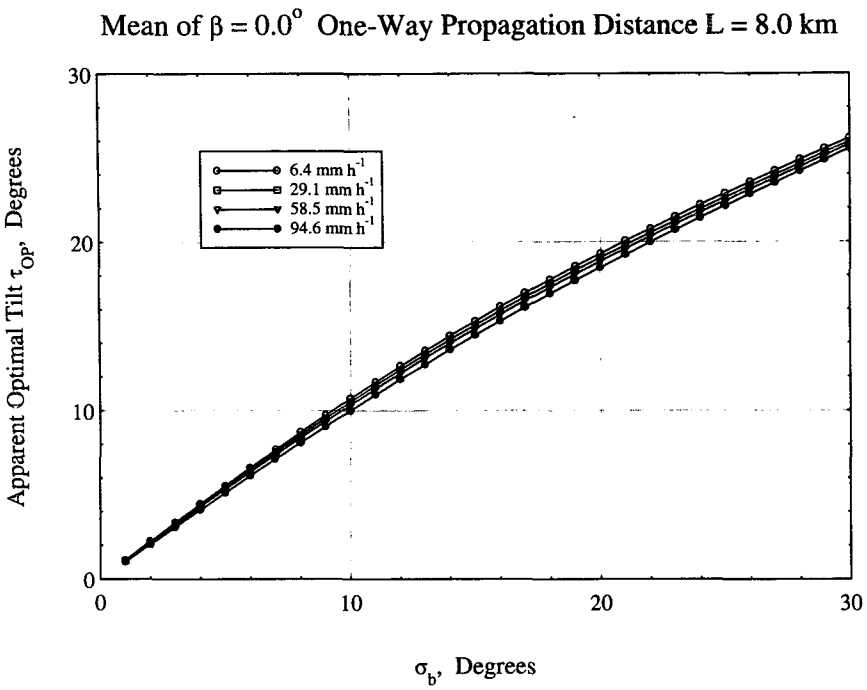

FIG. 10. The apparent optimal tilt τ_{op} versus the standard deviation of the canting angle distribution σ_β for the same four rain rates as in Fig. 9. Again $\bar{\beta} = 0°$, but the one-way propagation distance $L = 8$ km. In comparison with Fig. 9, the tilt is no longer completely insensitive to rain rate but the curves are still separated by less then 1°. The propagation phase spreads out the curves slightly.

average because just as many drops will cant positively as will cant negatively. In order to connect the measurements to calculations presented in this paper, each element in the series can be squared, the results added, and the square root taken to yield the rms values. Thus, the three polarization parameters can be defined in terms of their time series as

$$\mathcal{A} = \left(\frac{1}{N}\sum_i \mathcal{A}_i^2\right)^{1/2}; \quad \tau_{op} = \left(\frac{1}{N}\sum_i \tau_{opi}^2\right)^{1/2};$$

$$\epsilon_{op} = \left(\frac{1}{N}\sum_i \epsilon_{opi}^2\right)^{1/2}.$$

Work is in progress to model such matrices and to process real measurements from a limited number of research radars having the necessary capabilities.

5. Summary

Our goal here has been to explore the feasibility of optimal polarizations as a tool for retrieval of microphysical information. Although rain has been used as a test medium for these new parameters, their usefulness is not restricted to it and the estimation of microphysical parameters from other hydrometeors such as wet or dry hail can be examined with the same tools. Perhaps the most significant contribution is a critical one: one has to be cautious in interpreting results when combining the concepts of a scattering matrix (operator) and rms-type power averaging because the angular sign information is lost and the optimal eigenvectors always end up with positive tilts.

It is found that the optimal polarization parameters (asymmetry ratio $\mathcal{A}$, apparent optimal tilt τ_{op}, and apparent optimal ellipticity ϵ_{op}) are related to the microphysical parameters of the ensemble of drops (the reflectivity-weighted mean axial ratio $\mathcal{R}$, the mean canting angle $\bar{\beta}$, the standard deviation σ_β, and the propagation differential phase ϕ). When propagation effects can be ignored, the polarization variables can be obtained by simply measuring the copolarized and cross-polarized powers. Furthermore, the asymmetry ratio can be viewed as a generalization of Z_{DR} because it combines Z_{DR} and LDR and it is unaffected by propagation phase.

The relationships are summarized here for an ensemble of drops with prescribed canting parameters.

- The asymmetry ratio $\mathcal{A}$ is a good indicator of $\mathcal{R}$. It is less sensitive to canting than Z_{DR} and it is independent of propagation effects. Also, in addition to Z_{DR}, it requires only one measurement (the cross-polarized power).

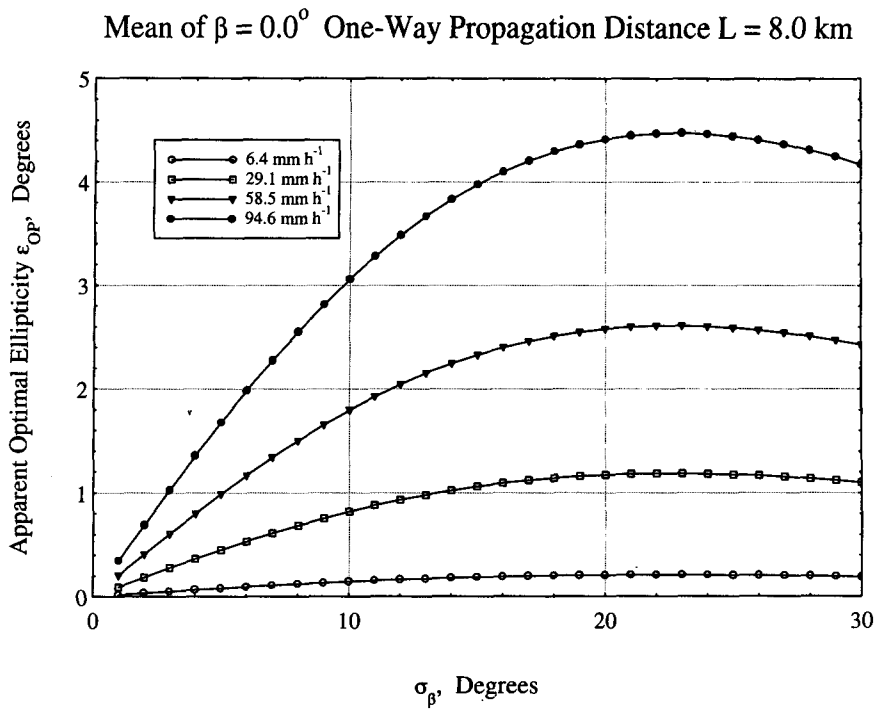

FIG. 11. The apparent optimal ellipticity ϵ_{op} versus σ_β for the same four rain rates as in Fig. 8. Again, $\bar{\beta} = 0°$ and the one-way propagation distance $L = 8$ km.

- In the absence of propagation effects, the apparent optimal tilt is not sensitive to rain rate and the optimal ellipticity is identically zero.
- The apparent optimal tilt τ_{op} is a function of $\bar{\beta}$, σ_β, and ϕ. Assuming $\bar{\beta} = 0$, however, the tilt depends on σ_β and ϕ only; that is, $\tau_{op} \rightarrow \tau_{op}(\sigma_\beta, \phi)$.
- The apparent optimal ellipticity ϵ_{op} is a function of $\bar{\beta}$, σ_β, ϕ. Assuming $\bar{\beta} = 0$, ϵ_{op} depends on σ_β and ϕ only; that is, $\epsilon_{op} \rightarrow \epsilon_{op}(\sigma_\beta, \phi)$.
- Both ϵ_{op} and τ_{op} exhibit a sinusoidal-type dependence on the propagation differential phase shift.

The asymmetry ratio gives a measure of the reflectivity-weighted mean axial ratio that is less affected by canting than would a measurement based on Z_{DR}. In fact, in the cases examined here, $\mathcal{A}$ seems to be better suited to measure microphysical characteristics. The only drawback is that the entire scattering matrix must be measured. This is not a serious problem, however, since several research radars have the ability to obtain the three average power measurements required for the rms scattering matrix at S band.[6]

The apparent optimal ellipticity and tilt are functions of both canting parameters and of propagation phase, but these dependencies can be considerably simplified under the assumptions given above. We are left with two measurables and two unknowns, and there is the possibility of recovering the standard deviation of the canting angle distribution and the propagation phase from ϵ_{op} and τ_{op} measurements.

We conclude by pointing out the limitations of our study. The differential attenuation was assumed negligible at S band, but in some cases, and certainly at smaller wavelengths, this is not a valid assumption. Possible effects of differential attenuation are discussed in appendix D. Backscatter differential phase shifts were also neglected in this work (S band), which may be invalid in scattering by, for example, large hail. Our preliminary calculations for X band (not included here) indicate that the backscatter phase does not significantly change the conclusions reported in this study.

Acknowledgments. One of us (JMK) would like to acknowledge NASA's support for this work given via the global change graduate student fellowship. Support for ABK was provided by the National Science Foundation Grant ATM-9116075. ARJ's contribution to this study was supported under Grant 958437 from JPL in support of the NASA SIR-C program. We would like to thank Larry Coke for streamlining, documenting, and modifying the *T*-matrix code originally developed by Waterman and later revised by Warner and Hizal. We would also like to thank J. Vivekanandan, D. Zrnić, and A. Ryzhkov for their helpful comments.

[6] Note that at higher frequencies $\mathcal{A}$ would also depend on the backscatter differential phase shift.

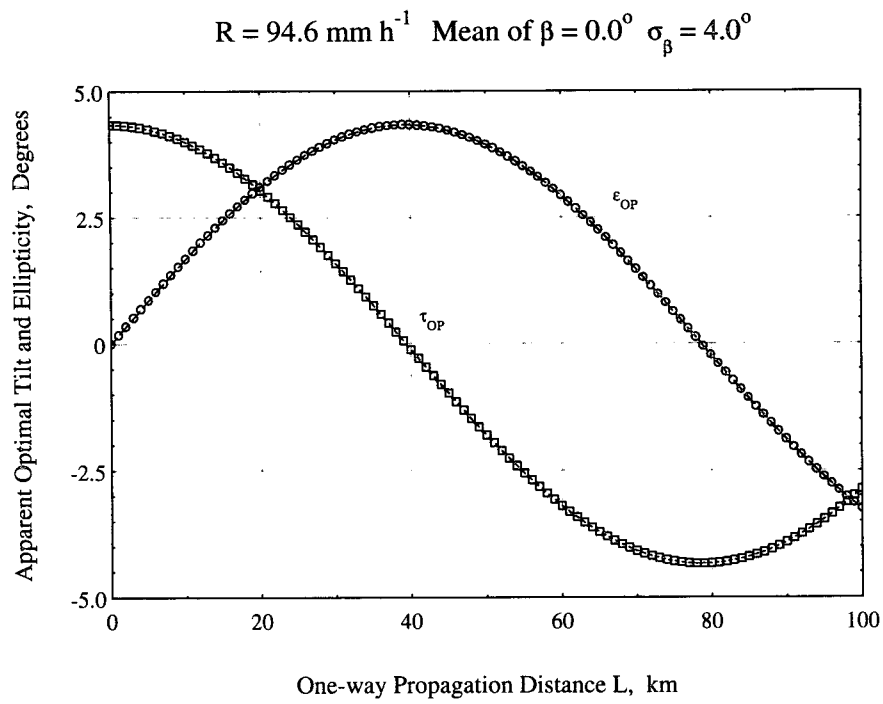

FIG. 12. The apparent optimal ellipticity ϵ_{op} and tilt τ_{op} versus the one-way propagation distance L (km). The mean canting angle $\bar{\beta} = 0°$, the standard deviation $\sigma_\beta = 4°$, and the rain rate $R = 94.6$ mm h^{-1}. The two polarization parameters exhibit a sinusoidal dependence on L. Note that while one is unlikely to ever encounter a one-way propagation path of 100 km in 94.6 mm h^{-1} rain, the propagation path is extended to this exaggerated value simply to illustrate the periodic dependence of ϵ_{op} and τ_{op} on L.

APPENDIX A

Polarimetric Definitions

Here basic definitions of radar polarimetry (Bringi and Hendry 1990; Ishimaru 1991; Kostinski et al. 1993), such as polarization vectors, the definition of the scattering matrix, and the optimal polarization technique are reviewed so that the eigenpolarizations can be related to the parameters of the polarization ellipse. These parameters are used to retrieve information about the hydrometeors.

a. Polarization vectors

The polarization of a plane electromagnetic wave is described using the polarization or Jones vector (e.g., Azzam and Bashara 1977; Born and Wolf 1980). This is a 2 × 1 complex vector and in a linear basis can be written as

$$\mathbf{E} = \frac{1}{(|E_x|^2 + |E_y|^2)^{1/2}} \begin{bmatrix} |E_x| \\ |E_y| e^{i\delta} \end{bmatrix}. \quad \text{(A1)}$$

The magnitudes of the x and y components are $|E_x|$ and $|E_y|$, respectively. The phase δ represents the phase difference between the x and y components of the wave. In this paper, we consider a linear basis consisting of horizontally $H(x)$ and vertically $V(y)$ polarized signals.

The polarization of the wave can also be described by a single complex number, χ (Azzam and Bashara 1977),

$$\chi = \frac{|E_y| e^{i\delta}}{|E_x|}, \quad \text{(A2)}$$

which is used to recover the parameters of the polarization ellipse (see, for example, appendix B). Both representations uniquely describe the polarization state of the wave.

The shape of the polarization ellipse itself (Fig. A1) can be specified by two parameters; ellipticity ϵ and tilt τ (Born and Wolf 1980; Azzam and Bashara 1977). The ellipticity is the "fatness" of the ellipse, and the tilt is the angle between the ellipse's major axis and the local horizontal. The original intent in introducing these parameters was probably to separate the shape and orientation of the polarization ellipse at the level of the wave (Born and Wolf 1980). It seems that such shape versus orientation decoupling is important at the scattering level as well because these parameters separate effects of particle shape from particle orientation. It therefore appears natural to express the eigenpolarizations in terms of ellipticity and tilt and to determine their dependence on such microphysical parameters as particle canting and shape.

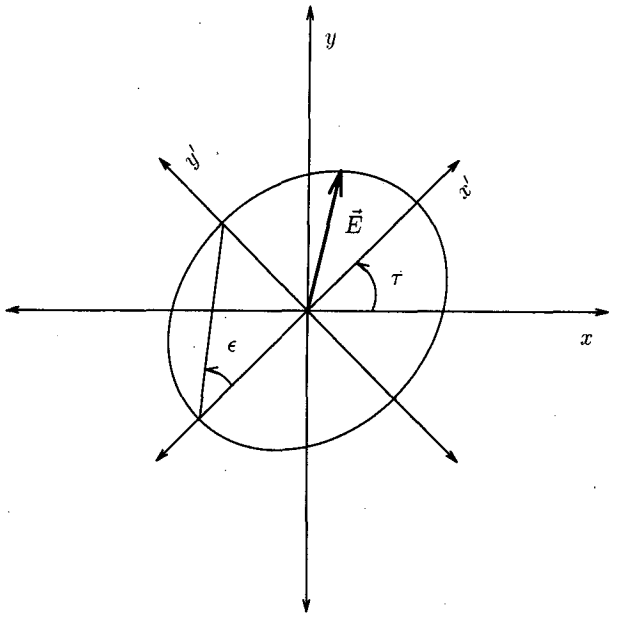

FIG. A1. General case of elliptical polarization for a complex electric field vector **E**. Ellipticity ϵ ("fatness" of the ellipse) and tilt τ (inclination of the major axis) are shown.

The ϵ and τ parameters have ranges of $-\pi/4 \leq \epsilon \leq \pi/4$ and $-\pi/2 \leq \tau \leq \pi/2$. They completely as well as uniquely describe all possible states of polarization. The sign of ϵ determines the sense of rotation of **E**, that is, right- or left-handed polarizations.[7]

b. Scattering matrix

The scattering of a polarized wave by a target can be described by a 2×2 complex scattering matrix acting on the 2D complex polarization vectors defined in the previous section. The scattering matrix can be written in a linear basis (e.g., Bohren and Huffman 1983; Ulaby and Elachi 1990) as

$$\mathbf{S} = \begin{bmatrix} S_{HH} & S_{HV} \\ S_{VH} & S_{VV} \end{bmatrix},$$

where each element consists of a magnitude and phase; that is, $S_{HH} = |S_{HH}|e^{i\delta_{HH}}$. The subscripts HH, HV, VH, VV represent the polarizations used to measure the matrix; that is, HH denotes a horizontal transmitted and received signal and the δ's with subscripts denote the corresponding phases.

It is advantageous to normalize the matrix by the (1, 1) element to give

$$\mathbf{S} = \begin{bmatrix} 1 & S_{HV}/S_{HH} \\ S_{VH}/S_{HH} & S_{VV}/S_{HH} \end{bmatrix}.$$

The overall phase δ_{HH} is not a measurable and can be set to zero. The phases in the matrix are now phase *differences* (relative to HH). To simplify the notation, the scattering matrix above is rewritten as

$$\mathbf{S} = \begin{bmatrix} 1 & be^{i\gamma} \\ be^{i\gamma} & ae^{i\delta} \end{bmatrix}, \tag{A3}$$

where a and b are magnitudes equal to $|S_{VV}|/|S_{HH}|$ and $|S_{VH}|/|S_{HH}|$, respectively. The phase γ represents the total phase difference between S_{HV} and S_{HH}, while δ is the total phase difference between S_{VV} and S_{HH}. At this point, no assumptions have been made about the physics of the scatterer, and (A3) is the most *general* form of the normalized symmetric scattering matrix.

APPENDIX B

Optimal Ellipticity and Tilt

Here a brief description of the method to obtain the optimal ellipticity and tilt from the eigenvectors of **G** is given. These parameters of the polarization ellipse are recovered from the eigenvectors of **G** by using χ as defined in (2). Note that this method is independent of the optimal polarization technique and can be used to obtain the ellipticity and tilt from a general polarization vector.

Given the graves matrix **G**, the eigenvalues and eigenvectors are found by solving

$$\mathbf{G}x = \lambda x \tag{B1}$$

(see, e.g., Strang 1988, chapter 5). Matrix **G** is obtained from **S** ($\mathbf{G} = \mathbf{S}^{\dagger}\mathbf{S}$), and in the case of a single canted drop, the elements of **S** are given in terms of the principal plane scattering amplitudes and the canting angle β [Eqs. (6)–(8)]. For a single canted drop, the two eigenvectors that satisfy (B1) are repeated here:

$$\mathbf{E}_1 = \frac{1}{(1 + \tan^2\beta)^{1/2}} \begin{bmatrix} 1 \\ \tan\beta \end{bmatrix};$$

$$\mathbf{E}_2 = \frac{1}{(1 + \cot^2\beta)^{1/2}} \begin{bmatrix} 1 \\ \cot\beta \end{bmatrix}.$$

The corresponding complex number representation of the polarizations are

$$\chi_1 = \tan\beta; \quad \chi_2 = \cot\beta. \tag{B2}$$

This complex number can be related to the ellipticity ϵ and tilt τ of the polarization ellipse by Azzam and Bashara (1977, p. 29):

$$\chi = \frac{\tan\tau + i\tan\epsilon}{1 - i\tan\tau\tan\epsilon}. \tag{B3}$$

When χ is real as is the case for our single canted drop, (B3) reduces to

[7] We note in passing that the helicity or handedness of the wave is defined here not only by the polarization vector (A1) but also by the direction of propagation (see, e.g., Collin 1985, p. 303).

$$\chi = \tan(\tau).$$

Consequently, the tilts of the two polarizations are found to be

$$\tau_1 = -\beta$$
$$\tau_2 = 90° - \beta.$$

The ellipticities are identically zero when χ is real.

In the general case of complex χ, the ellipticity and tilt can be recovered using Azzam and Bashara (1977, 33–34):

$$\tan 2\tau = \frac{2\,\mathrm{Re}(\chi)}{1 - |\chi|^2} \tag{B4}$$

$$\sin 2\epsilon = \frac{2\,\mathrm{Im}(\chi)}{1 + |\chi|^2}. \tag{B5}$$

Here Re and Im denote the real and imaginary parts of χ, respectively.

APPENDIX C

Symbolic Calculations

The use of symbolic software provides the opportunity to examine the explicit dependence of the optimal polarizations ϵ_{op} and τ_{op} on the elements of the scattering matrix **S**. Here we outline the steps that produce the optimal ellipticity as a function of the three variables a, b, and ϕ in the scattering matrix. The expression for **S** [Eq. (1)] is repeated here for convenience:

$$\mathbf{S} = \begin{bmatrix} 1 & be^{i\phi/2} \\ be^{i\phi/2} & ae^{i\phi} \end{bmatrix}.$$

First, the Graves matrix is determined from **S** (**G** = $\mathbf{S}^{\dagger}\mathbf{S}$). From G we then determine the eigenvalues and eigenvectors in terms of a, b, and ϕ. The asymmetry ratio $\mathcal{A}$ can then be expressed from the eigenvalues as

$$\mathcal{A} = \frac{(a+1)[4b^2 + (a-1)^2]^{1/2} + 2b^2 + a^2 + 1}{-(a+1)[4b^2 + (a-1)^2]^{1/2} + 2b^2 + a^2 + 1}. \tag{C1}$$

Note that this expression is independent of ϕ.

To determine the ellipticity, the complex polarization parameter χ is found for both the minimal and maximal polarization vectors. The ellipticity can then be obtained from χ using Azzam and Bashara (1977):

$$\epsilon = \frac{1}{2}\sin^{-1}\left[\frac{2\,\mathrm{Im}(\chi)}{1 + |\chi|^2}\right]. \tag{C2}$$

The explicit expression for ϵ_{op} as given in terms of the elements of $\mathbf{S}_{rms}$ is

$$\epsilon_{op} = \frac{1}{2}\sin^{-1}\left(\frac{c}{d}\sin\frac{\phi}{2}\right). \tag{C3}$$

The values of c and d depend only on the magnitudes of the copolarized and cross-polarized components of **S** and are given as

$$c = [4b^2 + (a-1)^2]^{1/2} + a - 1$$
$$d = b\left\{\frac{(a-1)[4b^2 + (a-1)^2]^{1/2} + 2b^2 + (a-1)^2}{2b^2} + 1\right\}.$$

While (C3) is not in general sinusoidal, it appears sinusoidal for $c/d < 1$. Typical values of c/d for S band are much less then unity. The argument of the sine function is simply $\phi/2$. In terms of the propagation path L and the rate of propagation phase shift Φ the argument becomes $L\Phi$. This relationship can be inverted to provide the propagation phase in terms of the optimal ellipticity

$$\phi = 2\sin^{-1}\left(\frac{d}{c}\sin 2\epsilon_{op}\right). \tag{C4}$$

APPENDIX D

Possible Effects of Attenuation

While differential attenuation caused by propagation has been ignored in this preliminary study, it might be significant in many realistic situations. Here we examine the effects of attenuation on the asymmetry ratio. It is well known that LDR is much more affected by the differential attenuation than Z_{DR} [and $\mathcal{A}$ depends on both through a and b; see Eq. (C1)]. Thus, in so far as differential attenuation affects LDR, the asymmetry ratio is also affected. Below we give a numerical illustration of the sensitivity of $\mathcal{A}$ to differential attenuation.

The data are taken from Bringi and Hendry (1990, Fig. 2.7, p. 162), where both Z_{DR} and LDR are plotted as a function of rainfall rate with propagation distance as a parameter. This plot was produced by assuming Marshall–Palmer raindrops with a Gaussian distribution of polar canting angles and $\sigma = 10°$. We have taken examples from the extreme cases of 1- and 20-km propagation distances using a rain rate of 30 mm h^{-1}.

At a propagation distance of 1 km, values of Z_{DR} and LDR are 1.625 and 1.3×10^{-3}, respectively. Note that the values are on a linear scale. At 20 km, Z_{DR} and LDR are 1.59 and 6.76×10^{-3}, respectively. The corresponding value of $\mathcal{A}$ [Eq. (C1)] at 1 km is 1.67 and at 20 km is 1.81. Observe that Z_{DR} changed by only 2%, while LDR changed by 135%. The corresponding change in $\mathcal{A}$ is 8%. It therefore appears that $\mathcal{A}$ is only slightly more sensitive to differential attenuation then Z_{DR} in spite of huge effects on LDR (an 8% versus 135% change).

REFERENCES

Aydin, K., and Y. Zhao, 1990: A computational study of polarimetric radar observables in hail. *IEEE Trans. Geosci. Remote Sens.*, **28**, 412–422.

Azzam, R. M. A., and N. M. Bashara, 1977: *Ellipsometry and Polarized Light.* North-Holland, 539 pp.

Barber, P. W., and S. C. Hill, 1990: *Light Scattering by Particles: Computational Methods.* World Scientific, 261 pp.

Battan, L. J., 1973: *Radar Observation of the Atmosphere.* The University of Chicago Press, 324 pp.

Beard, K., and A. Jameson, 1983: Raindrop canting. *J. Atmos. Sci.,* **40,** 448–453.

Bohren, C., and D. Huffman, 1983: *Absorbtion and Scattering of Light by Small Particles.* Wiley, 530 pp.

Born, M., and E. Wolf, 1980: *Principles of Optics.* 6th ed. Pergamon Press, 808 pp.

Bringi, V. N., and A. Hendry, 1990: Technology of polarization diversity radars for meteorology. *Radar Meteorology,* D. Atlas, Ed., Amer. Meteor. Soc., pp. 153–190.

——, T. A. Seliga, and S. M. Cherry, 1983: Statistical properties of the dual-polarization differential reflectivity (Z_{DR}) radar signal. *IEEE Trans. Geosci. Remote Sens.,* **GE-21,** 215–220.

Chandrasekar, V., J. Hubbert, V. Bringi, and P. Meischner, 1993: Transformation of dual polarized radar data via the instantaneous scattering matrix. Preprints, *26th Int. Conf. Radar Meteorology,* 118–120.

Collin, R. E., 1985: *Antennas and Radiowave Propagation.* McGraw-Hill, 508 pp.

Doviak, R. J., and D. S. Zrnić, 1993: *Doppler Radar and Weather Observations.* Academic Press, 562 pp.

Graves, C., 1956: Radar polarization power scattering matrix. *Proc. IRE,* **44,** 248–252.

Holt, A. R., 1984: Some factors affecting the remote sensing of rain by polarization diversity radar in the 3 to 35-GHz frequency range. *Radio Sci.,* **19,** 1399–1412.

——, 1992: Towards an understanding of the effects of propagation through rain on data from polarization diversity radars. *Direct and Inverse Methods in Radar Polarimetry.* W. Boerner, H. Brand, L. Cram, and W. Holm, Eds., Kluwer, 1679–1712.

Hubbert, J., V. Chandrasekar, V. Bringi, and P. Meischner, 1993: Processing and interpretation of coherent dual-polarized radar measurements. *J. Atmos. Oceanic Technol.,* **10,** 155–164.

Huynen, J. R., 1978: Phenomenological theory of radar targets. *Electromagnetic Scattering* P. L. E. Uslenghi, Ed., Academic Press, 653–712.

Ishimaru, A., 1991: *Propagation, Scattering, and Radiation of Electromagnetic Waves.* Academic Press, 637 pp.

Jameson, A. R., 1983: Microphysical interpretation of multiparameter radar measurements in rain. Part 1: Interpretation of polarization measurements and estimation of raindrop shapes. *J. Atmos. Sci.,* **40,** 1792–1802.

——, 1985a: Deducing the microphysical character of precipitation from multiple-parameter radar polarization measurements. *J. Climate Appl. Meteor.,* **24,** 1037–1047.

——, 1985b: Microphysical interpretation of multiparameter radar measurements in rain. Part III: Interpretation and measurement of propagation differential phase shift between orthogonal linear polarizations. *J. Atmos. Sci.,* **42,** 607–614.

——, 1986: Corrigendum to "On deducing the microphysical character of precipitation from multiple-parameter radar polarization measurements." *J. Climate Appl. Meteor.,* **25,** 1075.

——, and D. B. Johnson, 1990: Cloud microphysics and radar. *Radar Meteorology,* D. Atlas, Ed., Amer. Meteor. Soc., 323–347.

Kostinski, A., and W.-M. Boerner, 1986: On foundations of radar polarimetry. *IEEE Trans. Antennas Propag.,* **34**(12), 1395–1404.

——, B. James, and W.-M. Boerner, 1988: Polarimetric matched filter for coherent imaging. *Can. J. Phys.,* **66,** 871–877.

——, J. M. Kwiatkowski, and A. Jameson, 1993: Spaceborne radar sensing of precipitation above an ocean surface: Polarization contrast study. *J. Atmos. Oceanic Technol.,* **10,** 736–751.

McCormick, G., and A. Hendry, 1975: Principles for the radar determination of the polarization properties of precipitation. *Radio Sci.,* **10,** 421–434.

Oguchi, T., 1977: Scattering properties of Pruppacher-and-Pitter form raindrops and cross polarization due to rain: Calculations at 11, 13, 19.3, and 34.8 ghz. *Radio Sci.,* **12,** 41–51.

Pruppacher, H., and K. Beard, 1970: A wind tunnel investigation of the internal circulation and shape of water drops falling at terminal velocity in air. *Quart. J. Roy. Meteor. Soc.,* **96,** 247–256.

Ray, P. S., 1972: Broadband complex refractive indices of ice and water. *Appl. Opt.,* **11,** 1836–1844.

Sauvageot, H., 1992: *Radar Meteorology.* Artech House, 366 pp.

Schroth, A., M. Chandra, and P. Meischner, 1988: A C-band coherent polarimetric radar for propagation and cloud physics research. *J. Atmos. Oceanic Technol.,* **5,** 803–822.

Sekhon, R., and R. Srivastava, 1971: Doppler radar observations of drop-size distributions in a thunderstorm. *J. Atmos. Sci.,* **28,** 983–994.

Seliga, T. A., and V. N. Bringi, 1976: Potential use of radar differential reflectivity measurements at orthogonal polarizations for measuring precipitation. *J. Appl. Meteor.,* **15,** 69–76.

——, and ——, 1978: Differential reflectivity and differential phase shift: Applications in radar meteorology. *Radio Sci.,* **13,** 271–275.

Strang, G., 1988: *Linear Algebra and its Applications.* 3d ed. Academic, 505 pp.

Ulaby, F. T., and C. Elachi, 1990: *Radar Polarimetry for Geoscience Applications.* The Artech House, 364 pp.

van de Hulst, H. C., 1981: *Light Scattering by Small Particles.* Dover, 470 pp.

Vivekanandan, J., W. Adams, and V. Bringi, 1991: Rigorous approach to polarimetric radar modeling of hydrometeor orientation distributions. *J. Appl. Meteor.,* **30,** 1053–1063.

Warner, C., and A. Hizal, 1976: Scattering and depolarization of microwaves by spheroidal raindrops. *Radio Sci.,* **11,** 921–930.

Waterman, P. C. 1965: Matrix formulation of electromagnetic scattering. *Proc. IEEE,* **53,** 805–812.

——, 1971: Symmetry, unitarity, and geometry in electromagnetic scattering. *Phys. Rev.,* **3,** 825–839.

Zrnić, D., Balakrishnan, N., Ziegler, C., Bringi, V., and Aydin, K., 1993: Polarimetric signatures in the stratiform region of a mesoscale convective system. *J. Appl. Meteor.,* **32,** 678–693.